Linewidth of higher harmonics in a nonisochronous auto-oscillator: Application to spin-torque nano-oscillators

M. Quinsat, V. Tiberkevich, D. Gusakova, A. Slavin, J. F. Sierra, U. Ebels, L. D. Buda-Prejbeanu, B. Dieny, M.-C. Cyrille, A. Zelster, and J. A. Katine

Phys. Rev. B **86**, 104418 — Published 13 September 2012

DOI: 10.1103/PhysRevB.86.104418

Linewidth of Higher Harmonics in a Non-Isochronous Auto-Oscillator: Application to Spin-Torque Nano-Oscillators

M. Quinsat,[1,2,*] V. Tiberkevich,[3] D. Gusakova,[2] A. Slavin,[3] J. F. Sierra,[2] U. Ebels,[2]
L. D. Buda-Prejbeanu,[2] B. Dieny,[2] M.-C. Cyrille,[1] A. Zelster,[4] and J. A. Katine[4]

[1] *CEA-LETI, MINATEC-Campus, 17 Rue des Martyrs, 38054 Grenoble, France*
[2] *SPINTEC, UMR CEA/CNRS/UJF-Grenoble 1/Grenoble-INP, INAC, Grenoble, F-38054*
[3] *Department of Physics, Oakland University, Rochester, Michigan 48309 USA*
[4] *Hitachi GST, 3403 Yerba Buena Road, San Jose, California 95135, USA*

(Dated: July 6, 2012)

In an isochronous auto-oscillator, where the auto-oscillation frequency f does not depend on the oscillation amplitude, the linewidth of the n^{th} harmonic is n^2 times larger than the linewidth of the main auto-oscillation mode. Here we present a theoretical description that predicts that the increase of the linewidth of higher harmonics with harmonic number n is substantially slower in the case of a non-isoschronous oscillator, where f depends strongly on amplitude. Using spin-torque nano-oscillators as an example of a non-isochronous oscillator, this description is confirmed numerically and experimentally. The presented model allows one to extract important nonlinear parameters of an auto-oscillator of any physical nature from the measurement of higher harmonic linewidths.

Auto-oscillating systems are ubiquitous in nature, and can be found in many branches of science, such as physics (electronics, optics, or mechanics), chemistry and biology [1]. Since auto-oscillators are nonlinear, they generate not only the main auto-oscillation frequency, but also higher harmonics of this frequency. In an auto-oscillating regime, the external phase noise (or timing jitter) broadens the spectrum of all the generated frequencies and determines the finite generation linewidths [1–3].

Many auto-oscillators (e.g. lasers) are *isochronous*, in a sense that their auto-oscillation frequency is independent of the amplitude, but there is an important class of *non-isochronous* auto-oscillators where generated frequencies depend on the auto-oscillation amplitude [3–5]. For example, the human heart, all the auto-oscillators exploiting ferromagnetic resonance and, in particular, the recently developed spin-torque nano-oscillators (STNO) [3–11] belong to this class.

The *non-isochronous* property (or nonlinearity of the auto-oscillation frequency) provides a mechanism to convert the amplitude noise into phase noise and creates an additional effective source of a non-white (correlated) phase noise that substantially broadens the generation linewidth [3–5]. The same property is responsible for the broadening of a frequency band of synchronization in an array of coupled auto-oscillators [3, 12], and, therefore, the quantitative information about the auto-oscillator nonlinear parameters that determine synchronization, modulation and other non-autonomous properties is of a crucial importance for applications. Usually, these parameters can be determined only from rather complicated time-resolved experiments [9, 10, 13] or from non-autonomous frequency-domain measurements involving additional external signals [14, 15].

In our current work we demonstrate that there is a significant difference between *isochronous* and *non-isochronous* auto-oscillators in the linewidth values of higher generation harmonic due to the nonlinearity of the generation frequency in the latter case. This difference provides a method to determine the intrinsic nonlinear parameters of the auto-oscillator, such as the nonlinear coefficient of linewidth broadening ν and the damping rate of the amplitude fluctuations Γ_p, that determine the non-autonomous auto-oscillator dynamics [3].

The general theory of the auto-oscillator linewidth for an *isochronous* auto-oscillator was developed in [2, 16]. It was shown in [2] that the phase variance $\Delta\phi^2$ of an auto-oscillator increases linearly with time τ ($\Delta\phi^2 \sim \tau$, corresponding to a "random walk" of phase), and that the generation line has a Lorentzian shape. Considering that the phase variance of the n^{th} harmonic is given by:

$$\Delta\phi_n^2 = n^2\Delta\phi^2 \,, \tag{1}$$

and, since the phase performs a "random walk" in the *isochronous* case ($\Delta\phi^2 \sim \tau$), it results that the spectrum of the n^{th} *isochronous* auto-oscillator harmonic has a Lorentzian shape with the linewidth [2]:

$$\Delta f_n^{iso} = n^2\Delta f_1^{iso} \,, \tag{2}$$

which is n^2 times larger than the fundamental linewidth Δf_1^{iso} (full width at half maximum FWHM).

We would like to note, that the linewidth of the n^{th} harmonic in a *passive (damped) isochronous nonlinear resonator* is determined by a different relation:

$$\Delta f_n^{res} = n\Delta f_1^{res} \,, \tag{3}$$

and is only n-times larger than the passive resonator linewidth Δf_1^{res} determined by the resonator damping.

In contrast with [2], in the case of a *non-isochronous* auto-oscillator [3] the shape of the generation line becomes non-Lorentzian [6], and the phase variance of the main frequency is a non-linear function of τ (see Eq. (6)

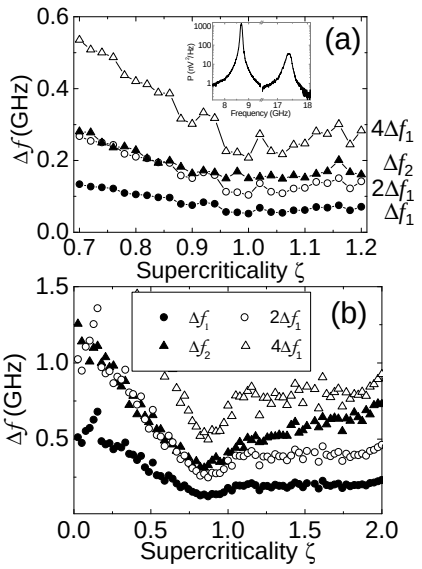

FIG. 1. FWHM Δf_1 and Δf_2 extracted from PSDs (a) for experiments on MTJs (sample A, nanopillar of 85nm diameter, resistance area product RA= $1\Omega.\mu m^2$, tunneling magnetoresistance TMR= 70%), (b) for macrospin simulations as in Ref. [9]. In the simulations the even (odd) harmonics were obtained from the PSD of the in-plane magnetization parallel (perpendicular) to the static equilibrium orientation. In (a) and (b) the Δf_2 values are compared with $2\Delta f_1$ (open circles) and $4\Delta f_1$ (open triangles). Inset in (a) : experimental PSD for $\zeta = 1.2$.

in [5]):

$$\Delta\phi_1^2(\tau) = 2\pi\Delta f_1^{iso}\left[(1+\nu^2)|\tau| - \nu^2\frac{1-e^{-2\Gamma_p|\tau|}}{2\Gamma_p}\right], \quad (4)$$

where Δf_1^{iso} is the linewidth of the main frequency in an *isochronous* auto-oscillator (in the absence of frequency nonlinearity), ν is the dimensionless coefficient characterizing the strength of this nonlinearity, and Γ_p is the damping rate of amplitude fluctuations in the auto-oscillation regime (for details see [3, 5]).

Obviously, the expression (2) will not hold in the non-isochronous case and the main goal of this work is to find a correct description for linewidth of the n^{th} harmonic in a non-isochronous auto-oscillator.

First of all, to illustrate the importance of this problem we demonstrate that the linewidth of higher harmonics in a non-isochronous auto-oscillator, indeed, deviates substantially from the well-known relation (2) established in Ref. [2].

A relevant example of a non-isochronous auto-oscillator that currently attracts a lot of attention from researchers is the STNO [3–11]. For STNOs multi-harmonic spectra of the steady-state oscillations were observed both in experiment and in simulations [11, 17].

In Fig. 1(a) we present the linewidth of a main auto-oscillation mode Δf_1 (filled circles) and the linewidth of its second harmonic Δf_2 (filled triangles) experimentally measured on a magnetic tunnel junction (MTJ) STNO as functions of the supercriticality parameter $\zeta = I/I_c$ defined as the ratio of the bias current I to its critical value I_c at which the auto-oscillation regime starts. In the same figure, we show for comparison values of $2\Delta f_1$ (open circles) and $4\Delta f_1$ (open triangles). The experimental linewidths were obtained from the Lorentzian fits of the power spectral density (PSD) of the magnetoresistive voltage signal acquired in the frequency domain (resolution bandwidth: 3MHz, experimental details can be found elsewhere [18]). An example of such a power spectrum is shown in the inset of Fig. 1(a) for $\zeta = 1.2$.

In Fig. 1(b) we present the results of numerical simulations of the magnetization dynamics in an STNO with parameters (same as in Ref. [9]) that are qualitatively similar to that of our experimental MTJ STNO (Fig. 1(a)), assuming that the dynamic magnetization in the STNO free layer is spatially uniform. In the framework of these "macrospin" simulations we performed numerical integration of the Landau-Lifshitz-Gilbert equation [19], where the Slonczewski spin torque term [20], as well as the Gaussian white noise term simulating the influence of thermal fluctuations [21], were included. In Fig. 1(b) the linewidth Δf_1 of the main mode is shown by the filled circles, the linewidth Δf_2 is shown by the filled triangles, while the calculated values $2\Delta f_1$ and $4\Delta f_1$ are shown by open symbols.

The simulations give a good qualitative description of the auto-oscillation modes observed experimentally in an STNO based on an MTJ. In both cases (experiment and simulation) the dynamics corresponds to the in-plane precession (IPP) mode of the in-plane magnetized free layer, whose static magnetization is anti-parallel to the static magnetization of the STNO pinned layer. While in the simulations harmonics up to the order $n = 7$ can be analyzed, in the experiment they are limited to $n = 2$.

The behavior of the linewidth Δf_2 of the second harmonic in our "macrospin" simulations, Fig. 1(b) is qualitatively similar to the behavior of Δf_2 in the experiment (see Fig. 1(a)) in both the subcritical and supercritical regime. In particular the second harmonic Δf_2 of the second harmonic in the subcritical ($\zeta < 1$) (or *passive resonator*) regime practically coincides with $2\Delta f_1$.

At the same time, it is clear from Fig. 1 that in the *auto-oscillation regime* ($\zeta > 1$) the linewidth of the second harmonic does not follow the predictions of the well-known theory [2], and that the experimental and numerical ratios of the second harmonic to the fundamental mode are smaller than expected from Eq. (2), but larger than expected from Eq. (3), i.e. they lie in the interval $2\Delta f_1 < \Delta f_2 < 4\Delta f_1$. To understand the qualitative reason of this discrepancy we present below an analytical derivation of the higher harmonics linewidth in a general non-isochronous auto-oscillator.

It has been shown in Ref. [3] that the complex ampli-

tude $c(t)$ of the oscillating variable in a non-isochronous auto-oscillator can be described by the equation:

$$\frac{dc}{dt} + i\omega(p)c + \Gamma_+(p)c - \Gamma_-(p)c = \xi(t)\ , \qquad (5)$$

where $p = |c|^2$ is the dimensionless oscillation power, $\omega(p)$ is the nonlinear oscillation frequency, $\Gamma_+(p)$ is the positive nonlinear damping, $\Gamma_-(p)$ is the negative damping (in the STNO it is caused by the spin-torque effect), and $\xi(t)$ is the stochastic process describing the influence of the white Gaussian noise. In the model (5) the steady auto-oscillations are excited when $\zeta \equiv \Gamma_-(0)/\Gamma_+(0) = 1$, i.e. at the point where negative damping compensates positive one at zero oscillation power. The complex amplitude of the n^{th} harmonic of the main oscillation mode excited in the auto-oscillator (5) is proportional to c^n.

In the subcritical regime $\zeta < 1$, the FWHM of a passive oscillator (or resonator) is determined by the positive linear damping $\Gamma_+(0)$. This regime can be easily analyzed using Eq. (5) linearized near $c = 0$ and all the nonlinearities of the STNO parameters in this regime are neglected. In this linear subcritical regime, Eq. (5) has the following analytic solution:

$$c_0(t) = \int_0^t \xi(t')exp[-(i\omega_0 + \Gamma_s)(t - t')]dt'\ , \qquad (6)$$

where $\omega_0 = \omega(0)$ is the frequency of linear oscillations and $\Gamma_s = \Gamma_+(0) - \Gamma_-(0) = (1 - \zeta)\Gamma_+(0)$ is the effective relaxation rate. The autocorrelation function $K_n(\tau) =< c^n(t+\tau)[c^*(t)]^n >$ of the n^{th} order harmonic can be easily found from the above expression and is an exponentially decaying function with $n\Gamma_s$ as the characteristic decay time:

$$K_n(\tau) = n!c_0^n exp(-n\Gamma_s\tau), \qquad (7)$$

where the mode amplitude c_0 is proportional to the noise power.

Two important properties follow from this equation. The first is that in the subcritical regime $\zeta < 1$ the lineshape of the main mode and all its harmonics is Lorentzian and that the corresponding linewidth of the n^{th} harmonic is related to the linewidth of the main mode by Eq. (3). This theoretical result is confirmed by both the simulations and experiment shown in Fig. 1 for the second harmonic. Here, it is clear that Eq. (3) holds up to the point $\zeta = 0.95$, where nonlinear terms in Eq. (5) become important.

The second important property is that the fundamental linewidth is given by the amplitude relaxation rate with $\Delta f_1 = \Gamma_s/\pi \propto (1 - \zeta)$. This result is confirmed by the almost linear decrease of the linewidth with ζ seen in Fig. 1.

In the supercritical regime, when the oscillation power substantially exceeds the noise level (this condition is typically satisfied for $\zeta > 1.05$), the amplitude fluctuations do not contribute *directly* to the correlation function $K_n(\tau)$, and it is determined solely by the phase decoherence, $K_n(\tau) \propto exp(-n^2\Delta\phi^2)$. For a non-isochronous oscillator, however, the amplitude fluctuations change the phase dynamics through the nonlinear amplitude-frequency coupling, and the phase variance $\Delta\phi^2$ is determined by Eq. (4) (see [3] and [5] for details).

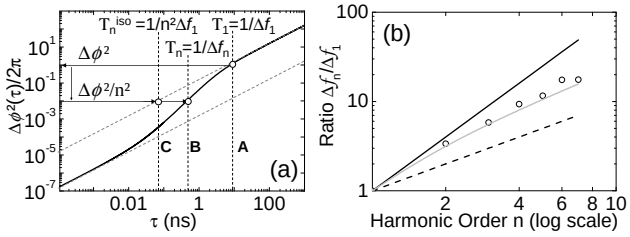

FIG. 2. (a) Calculated phase variance $\Delta\phi^2(\tau)$ from Eq. (4) using $\Delta f_0 = 10$MHz, $1/\Gamma_p = 3.18$ns and $\nu = 10$. Point A corresponds to $1/\Delta f_1$, Point B corresponds to the expected coherence time $(1/\Delta f_n)$ for the n=10 harmonic for the non-isochronous oscillator and point C corresponds to the isochronous oscillator; (b) Ratio $\Delta f_n/\Delta f_1$ versus harmonic order n from simulations. Black dashed and solid lines are for $\Delta f_n = n\Delta f_1$ and $\Delta f_n = n^2\Delta f_1$, respectively. The gray line shows is the values calculated from Eqs. (4), (8) with the non-linear parameters Γ_p and ν extracted from the first harmonic signal. Dots are the results of a "macrospin" numerical simulation performed for $\zeta = 1.8$.

The phase variance Eq. (4) is plotted in Fig. 2(a) for typical STNO parameters. One can distinguish three regimes. For long time scales $\tau >> 1/2\Gamma_p$ and for short time scales $\tau << 1/(2\Gamma_p\nu^2)$ the phase variance is linear in τ, while in between the phase variance is quadratic in τ [5].

To find the generation linewidth Δf_n from the phase variance $\Delta\phi^2$ one should, in principle, find the generation spectrum as a Fourier image of the correlation function $K_n(\tau)$, which cannot be done analytically. It is clear, however, that at the correlation time $T_n = 1/\Delta f_n$ the value of the n^{th} harmonic phase variance $n^2\Delta\phi^2(T_n)$ should be of the order of unity. Our calculations show that a good estimation of the linewidth can be obtained from the following simple relation:

$$\Delta\phi^2(T_n) = 2\pi/n^2\ . \qquad (8)$$

Eq. (8) gives an *exact* value of the linewidth Δf_n for a random-walk process $\Delta\phi^2 \sim \tau$, and its error does not exceed 6% in the quadratic region $\Delta\phi^2 \sim \tau^2$.

Combining Eqs. (4) and (8), one can easily understand why for a non-isochronous oscillator the linewidths Δf_n deviate from the well-known relation (2). The fundamental linewidth Δf_1 corresponds to the coherence time $T_1 = 1/\Delta f_1$ for which the phase variance is $\Delta\phi^2(T_1 = 1/\Delta f_1) = 2\pi$ (line A in Fig. 2(a)). The linewidth Δf_n of the n^{th} harmonic is, then, found as the inverse of the

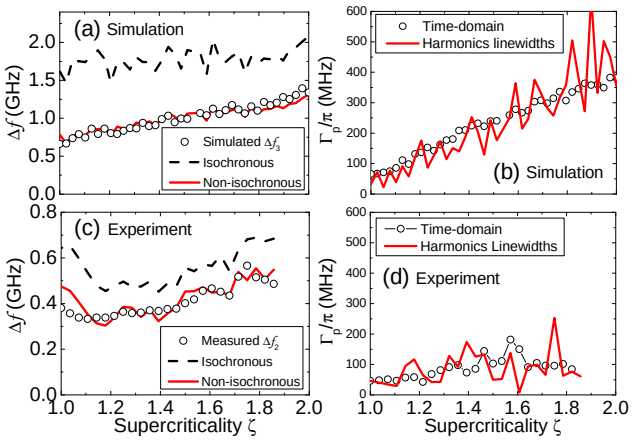

FIG. 3. (Color on-line) Verification of the method based on the higher harmonic linewidths. Linewidth of the n^{th} harmonic (shown by open dots) extracted from the time-domain data ((a)-numerically simulated for $n = 3$, (c)-experimentally measured for $n = 2$) in comparison with the analytical results for isochronous ([2]) and non-isochronous (Eq.(8)) models. Results from model [2] are shown by the dashed line, while results from Eq.(8) are shown by the continuous red line; Nonlinear parameter Γ_p (shown by open dots) extracted from the time-domain data ((b)-numerically simulated, (d)-experimentally measured) in comparison with the same parameter calculated using Eq.(8) from the calculated or measured values of Δf_1, Δf_2 and ν. Note, that a different MTJ device was used in the experiments Fig. 3(c) and Fig.3(d) compared to Fig.1(a).

coherence time $T_n = 1/\Delta f_n$ for which the phase variance is $2\pi/n^2$ (line B in Fig. 2(a)). It can be seen immediately that the corresponding coherence time in the case of a non-isochronous oscillator (line B) is larger than for an isochronous one (line C), whose phase variance is linear in time for all time scales (pure random walk phase). Correspondingly, the linewidths of higher harmonics are smaller than predicted by Eq. (2) with $\Delta f_n < n^2 \Delta f_1$. Moreover, since the logarithmic slope of $\Delta\phi^2(\tau)$ changes between 1 ($\Delta\phi^2 \sim \tau$) and 2 ($\Delta\phi^2 \sim \tau^2$), for a general non-isochronous oscillator the linewidth Δf_n always lies in the interval $n\Delta f_1 < \Delta f_n < n^2 \Delta f_1$ as has been found in experiment and in simulations, Fig. 1. By fitting the experimental (or numerically calculated) dependence $\Delta f_n(n)$ using (8) it is possible to determine the nonlinear auto-oscillator parameters ν and Γ_p. Thus, Eq. (8) and the above presented analysis constitute the main theoretical result of this paper.

In order to further verify the presented theoretical description, we compare the linewidth of the higher harmonics obtained from a Lorentzian fit of the numerically calculated PSD (open dots in Fig. 3(a,c)) to the results obtained from the analytical model (4), (8) (red lines in Fig. 3(a,c)). For the analytical model the non-linear parameters ν and Γ_p of the auto-oscillator were extracted in each case independently from the phase and amplitude noise of the first harmonic (fundamental frequency) following [9, 13], and the intrinsic linewidth Δf_0 was calculated from Eq. (4) for Δf_1. Using the set of values $\Gamma_p, \nu, \Delta f_0$, obtained solely from the analysis of the signal at the fundamental frequency, we then calculated Δf_n from Eqs. (4) and (8) to obtain the continuous red lines in Fig. 3. One can see that the model (4), (8) gives a good description of Δf_n in the auto-oscillation regime $\zeta > 1$, as shown in Fig. 3(a) for the 3^{rd} harmonic obtained from macrospin simulations and in Fig. 3(c) for the 2^{nd} harmonic measured experimentally. In Fig. 2(b), this is shown more explicitly for the macrospin simulation for orders $n = 2$ to 7. In contrast to the non-isochronous model Eq. (8) (red lines) the well-known model of an isochronous auto-oscillator [2] (black dashed line, see also Eq.(1) above) does not provide an adequate description of the higher order harmonic linewidths.

An important consequence of the above developed non-isochronous model (8) is that by measuring experimentally the linewidths of three harmonics in a non-isochronous auto-oscillator it is possible to extract via the analytical model (4), (8) the three parameters Γ_p, ν and Δf_0 that define many properties of the dynamics of the system (see Fig. 3(b,d), where the values of the nonlinear STNO parameter Γ_p, determined from the time-domain data are compared with the values of the same parameter determined from the higher harmonics linewidths data using the model (8)). This method of extraction of the nonlinear auto-oscillator parameters is very general and can be used for auto-oscillators of different physical nature in a wide range of auto-oscillation amplitudes (or supercriticalities ζ). It will be of particular importance when the time domain data from the auto-oscillator (e.g. used in Ref. [9, 10, 13]) are not available.

In conclusion, we have provided a general analytical description for the linewidth Δf_n of higher harmonics in a non-isochronous auto-oscillator. Using this analytical description it is possible to determine all the nonlinear parameters of a non-isochronous auto-oscillator if the linewidths of at least three generated harmonics are experimentally measured or numerically calculated. Using these parameters it is possible to theoretically predict the non-autonomous behavior of the auto-oscillator [3].

This work was supported in part by the French national research agency (ANR) through ANR-09-NANO-037 and the Carnot-RF project and Nano2012 convention. J. F. Sierra acknowledges support from the FP7-People-2009-IEF program no 252067. Oakland University group is supported by the National Science Foundation grant ECCS-1001815, by the grant from DARPA, and by the grants from U.S. Army TARDEC, RDECOM.

* michael.quinsat@cea.fr

[1] M. I. Rabinovich and D. I. Trubetskov, *Oscillations and Waves in Linear and Nonlinear Systems* (Boston, MA: Kluwer, 1989).

[2] A. Demir, A. Mehrotra, and J. Roychowdhury, IEEE Transactions on Circuits and Systems I: Fundamental Theory and Applications **47**, 655 (2000).

[3] A. Slavin and V. Tiberkevich, IEEE TRANSACTIONS ON MAGNETICS **45**, 1875 (2009).

[4] J.-V. Kim, V. Tiberkevich, and A. N. Slavin, Phys. Rev. Lett. **100**, 017207 (2008).

[5] V. S. Tiberkevich, A. N. Slavin, and J.-V. Kim, Phys. Rev. B **78**, 092401 (2008).

[6] J.-V. Kim, Q. Mistral, C. Chappert, V. S. Tiberkevich, and A. N. Slavin, Phys. Rev. Lett. **100**, 167201 (2008).

[7] C. Boone, J. A. Katine, J. R. Childress, J. Zhu, X. Cheng, and I. N. Krivorotov, Phys. Rev. B **79**, 140404 (2009).

[8] K. Kudo, T. Nagasawa, R. Sato, and K. Mizushima, Journal of Applied Physics **105**, 07D105 (2009).

[9] M. Quinsat, D. Gusakova, J. F. Sierra, J. P. Michel, D. Houssameddine, B. Delaet, M.-C. Cyrille, U. Ebels, B. Dieny, L. D. Buda-Prejbeanu, J. A. Katine, D. Mauri, A. Zeltser, M. Prigent, J.-C. Nallatamby, and R. Sommet, Applied Physics Letters **97**, 182507 (2010).

[10] M. W. Keller, M. R. Pufall, W. H. Rippard, and T. J. Silva, Phys. Rev. B **82**, 054416 (2010).

[11] S. I. Kiselev, J. Sankey, I. Krivorotov, N. Emley, R. Schoelkopf, R. Buhrman, and D. Ralph, Nature **425**, 380 (2003).

[12] A. Pikovsky, M. Rosenbblum, and J. Kurths, *Synchronization: A Universal Concept in Nonlinear Sciences* (Cambridge, New York, 2001).

[13] L. Bianchini, S. Cornelissen, J.-V. Kim, T. Devolder, W. van Roy, L. Lagae, and C. Chappert, Applied Physics Letters **97**, 032502 (2010).

[14] J. Sankey, P. Braganca, A. G. F. Garcia, I. N. Krivorotov, R. A. Buhrman, and D. C. Ralph, , 227601.

[15] S. Urazhdin, V. Tiberkevich, and A. Slavin, 10.1103/PhysRevLett.105.237204.

[16] K. Kurokawa, IEEE TRANSACTIONS ON MICROWAVE THEORY AND TECHNIQUES **MTT-16**, 234 (1968).

[17] S. E. Russek, S. Kaka, W. H. Rippard, M. R. Pufall, and T. J. Silva, Phys. Rev. B **71**, 104425 (2005).

[18] M. Quinsat, J. F. Sierra, I. Firastrau, V. Tiberkevich, A. Slavin, D. Gusakova, L. D. Buda-Prejbeanu, M. Zarudniev, J.-P. Michel, U. Ebels, B. Dieny, M.-C. Cyrille, J. A. Katine, D. Mauri, and A. Zeltser, Applied Physics Letters **98**, 182503 (2011).

[19] D. Gusakova, M. Quinsat, J. F. Sierra, U. Ebels, B. Dieny, L. D. Buda-Prejbeanu, M.-C. Cyrille, V. Tiberkevich, and A. N. Slavin, Applied Physics Letters **99**, 052501 (2011).

[20] J. C. Slonczewski, Journal of Magnetism and Magnetic Materials **159**, L1 (1996).

[21] W. F. Brown, Phys. Rev. **130**, 1677 (1963).